Evaluation of Low-Exergy Heating and Cooling Systems and Topology Optimization for Deep Energy Savings at the Urban District Level

Amy Allen[a,b,*], Gregor Henze[a,b,c], Kyri Baker[a,b,c], Gregory Pavlak[d]

[a] *University of Colorado, UCB 428, Boulder, Colorado, 80309, United States*
[b] *National Renewable Energy Laboratory, 15013 Denver West Parkway, Golden, Colorado, 80401, United States*
[c] *Renewable and Sustainable Energy Institute, 027 UCB Suite N321, Boulder, Colorado, 80309, United States*
[d] *Pennsylvania State University, 104 Engineering Unit A, University Park, Pennsylvania, 16802, United States*

Abstract

District energy systems have the potential to achieve deep energy savings by leveraging the density and diversity of loads in urban districts. However, planning and adoption of district thermal energy systems is hindered by the analytical burden and high infrastructure costs. It is hypothesized that network topology optimization would enable wider adoption of advanced (ambient temperature) district thermal energy systems, resulting in energy savings. In this study, energy modeling is used to compare the energy performance of "conventional" and "advanced" district thermal energy systems at the urban district level, and a partial exhaustive search is used to evaluate a heuristic for the topology optimization problem. For the prototypical district considered, advanced district thermal energy systems mated with low-exergy building heating and cooling systems achieved a source energy use intensity that was 49% lower than that of conventional systems. The minimal spanning tree heuristic was demonstrated to be effective for the network topology optimization problem in the context of a prototypical district, and contributes to mitigating the problem's computational complexity. The work presented in this paper demonstrates the potential of advanced district thermal energy systems to achieve deep energy savings, and advances to addressing barriers to their adoption through topology optimization.

Keywords: Fifth-generation district heating and cooling systems, topology analysis, hydraulic network modeling

1. Introduction

Governing bodies worldwide have recognized the importance of reducing carbon emissions. Beneficial electrification of energy end uses, in conjunction with decarbonization of electricity generation, is widely recognized as a critical strategy to accomplish this goal [1]. Electrification of transportation has made promising strides in this direction, but

*Corresponding author

Email addresses: amy.allen@colorado.edu (Amy Allen), Gregor.Henze@colorado.edu (Gregor Henze), Kyri.Baker@colorado.edu (Kyri Baker), gxp93@psu.edu (Gregory Pavlak)

space heating and cooling pose greater challenges. In 2016, the European Union introduced a Heating and Cooling Strategy which seeks to promote decarbonization of space heating and cooling, and greater utilization of industrial waste heat [2]. In this context, the potential of low-exergy heating, ventilation and air-conditioning (HVAC) systems, which are compatible with electrically-driven primary heating and cooling equipment, and the beneficial use of waste heat, is demonstrated as a strategy to accomplish electrification of space heating and cooling. However, these systems require district thermal energy networks, which are expensive to build and difficult to screen for cost-effectiveness. Expansion of the use of district thermal energy systems in the context of increased penetration of renewable electricity generation will require new analysis tools capable of addressing integrated thermal and electrical systems [3]. Specifically, selecting the best network topology for a district thermal energy system is a key challenge, in both retrofits and new construction. A topology optimization framework is proposed to address this problem.

The work presented in this paper is part of a larger effort to develop a framework for topology optimization of district thermal energy systems, which seeks to answer the questions, for a given urban district, "Which subset of buildings, if any, are most advantageous to connect to a district thermal energy system, and by what network topology should they be connected, in order to minimize life cycle cost?" The work presented in this paper demonstrates the potential of advanced district thermal energy systems to achieve deep energy savings, and steps to addressing barriers to their adoption through network topology optimization. This paper presents results from a comparison of "conventional" and "advanced" district thermal energy systems at the level of a low-energy urban district, and an evaluation of a heuristic for part of the topology optimization problem.

1.1. Advanced district thermal energy systems

In this work, the term "advanced" district thermal energy systems will be used to encompass fifth generation district heating and cooling systems, ambient loops, and other moderate-temperature district networks. The evolution of district thermal energy systems over their 140 years of existence has often been characterized in terms of generations (with most authors recognizing either four or five generations), with the defining feature being a progression from steam to hot water for heating, and to more moderate temperatures of water for both heating and cooling [4].

The work of [5] introduced the concept of "deep energy savings" in the context of design strategies that address interactive effects among multiple building systems to achieve significant reductions in energy use. In this work, the concept of deep energy savings is extended to systems implemented at the urban district level. Advanced district thermal energy systems have the potential to achieve deep energy savings by leveraging the density and diversity of loads in urban districts [6]. An analysis found that wide-scale expansion of district heating, in conjunction with building energy efficiency, would allow the European Union to achieve its target for reducing carbon emissions 80% from 1990 levels by 2050, at a 15% lower cost than through energy efficiency strategies at the individual building level alone [7]. The work of [4] identified factors that allow advanced systems to save energy and reduce carbon emissions relative to conventional district thermal energy systems. Moderate water temperatures facilitate the integration of waste heat sources (including through combined heat and power), and renewable heat sources, such as solar thermal and geothermal. Reduced supply temperatures in heating facilitate the use of heat pumps and condensing boilers, and warmer supply temperatures in cooling increase the potential for water-side economizing, reducing the energy intensity of the primary equipment. The use of electric heat pumps in place of natural gas-fired boilers is compatible with decarbonization of source energy and a transition to 100% renewable energy [3]. Moderate water temperatures also reduce undesired heat losses and gains in the distribution system [4]. Advanced district thermal energy systems can also be leveraged for beneficial grid interactivity, such as through the use of "excess" renewable electric generation to charge thermal energy storage [8].

This work will focus on so-called "fifth generation district heating and cooling (5GDHC) systems." The work of [9] defines a 5GDHC system as a thermal energy network circulating water or brine that leverages water source heat pumps to temper the supply fluid at the connected loads. A study of operating 5GDHC systems found that most had network temperatures in the range of 15-25°C [9]. In the analysis of the topology optimization problem in this study, a 5GDHC system with a two-pipe configuration, permitting bidirectional thermal and mass flow, is considered, with buildings connected in parallel to the thermal network. Each connected building is equipped with an energy transfer station (ETS), consisting of a heat pump, a heat exchanger, and a distribution pump. The heat pump in the ETS will temper the water from the district energy network as required for the building's load. Based on the building's load, the distribution pump or pumps will draw water either from the system's "cool pipe" or "warm pipe." A schematic representation of this system is shown in Fig 1.

1.2. Low-exergy building systems

The benefits of the use of more moderate water temperatures by advanced district thermal energy systems can be characterized in terms of their lower exergy requirements compared with conventional district thermal energy systems. The concept of exergy combines the first and second laws of thermodynamics, and refers to the maximum work obtained if a system is brought into thermodynamic equilibrium with its environment [11]. To maximize the exergetic efficiency, advanced district thermal energy systems must be paired with low-exergy HVAC systems at the building level, of which radiant hydronic HVAC systems are one example [12]. Low-exergy hydronic HVAC systems are characterized by lower temperature differentials between both supply water temperatures and outdoor air temperatures, and supply water temperatures and zone air temperatures, which allow for lower-lift operation of chillers and heat pumps and reduce distribution losses [13].

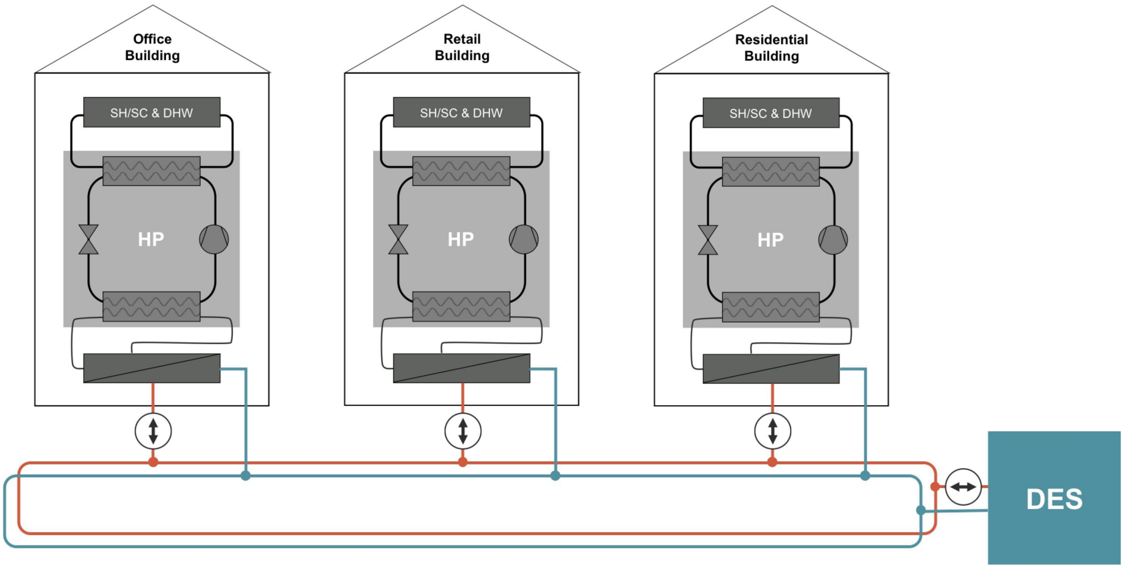

Figure 1: Schematic representation of 5GDHC system, courtesy of [10]

Radiant heating and cooling systems transfer and reject heat to a conditioned space through both radiation and convection. Specifically, radiant heating and cooling systems have been defined as HVAC systems that transfer more than 50% of their total heat flux by thermal radiation [14]. In this work, radiant hydronic thermo-active building systems (TABS), specifically, hydronic coils embedded in concrete slab floors, will be analyzed. These types of systems are considered "thermo-active" because building components, in this case, mass floors, are charged and discharged with thermal energy, which is then transferred to (or absorbed from) the conditioned space through convection and radiation [12]. Radiative transfer with the active heated and cooled surface can increase the differential between inside and outside surface temperatures for the non-activated zone surfaces [15]. A high-performance building envelope mitigates this effect and minimizes an increase in conductive heat transfer for the non-activated surfaces, making low-exergy HVAC systems particularly well suited to buildings with high-performance envelope designs and limited cooling load densities, such as those considered in this study. Due to their different operating mechanisms, load profiles differing in both timing and magnitude would be observed on radiant hydronic and air-based HVAC systems conditioning the same space [16]. In assessing energy performance of radiant hydronic systems, it is important to consider heat transfer at both the surface level and the hydronic loop level. Due to the thermal mass inherent in TABS, the peak rate of surface heat removal or addition is expected to be different from the peak rate of heat removal or addition to the hydronic loop [16]. In sizing radiant hydronic systems, the peak loads imposed on the hydronic loop are generally the relevant parameter [16]. Several studies analyzing radiant hydronic systems at the building level have found the peak cooling loads observed by radiant systems to be higher than those observed by air-based systems [17]. In a simulation study of air-based and radiant hydronic HVAC systems in the form of TABS, in which ventilation and latent loads were not considered, the peak surface cooling rate was found to be 23% to 84% higher, and the peak hydronic cooling rate, 33% to 70% higher, than the peak cooling loads for an air-based system. The wide variation reflects variation in several parameters, including solar heat gain, level of envelope thermal insulation, radiative/convective split associated with internal gains, and orientation of the radiant surface (ceiling or floor) [16]. Another comparison study of air-based and radiant hydronic HVAC systems, in which the radiant systems were coupled with an air system to supply ventilation air, found comparable peak cooling loads between the two system types, with the radiant system having a higher annual cumulative cooling load. The higher annual cooling load for the radiant system was attributed to a higher level of thermal comfort in cooling mode being provided [12].

Radiant hydronic and air-based HVAC systems are generally controlled by different mechanisms, making a direct comparison of the two system types challenging [15]. Due to their thermal inertia, TABS cannot respond quickly to changes in load or setpoint [12]. Air-based HVAC systems are generally controlled to air temperature, and in practice, radiant hydronic HVAC systems can be controlled based on surface temperature, water temperature, or other parameters [15]. Controlling the radiant system to operative temperature and controlling the air-based system to the sequence of operative temperatures that results in the space conditioned by the radiant system, is one approach that has been used in other simulation studies comparing the two system types [16]. Operative temperature is defined as the average of the mean radiant temperature of the zone surfaces and the air temperature and is a key factor in influencing human thermal comfort [12]. Through their use of heated or cooled surfaces, radiant HVAC systems can achieve a comparable level of thermal comfort to air-based systems at lower air temperatures in heating, and higher air temperatures in cooling [17].

1.3. District-scale energy analysis

In performing energy simulation of urban districts, to avoid modeling each building individually, archetypal buildings are often selected to represent either specific existing buildings, or typical buildings of the type that are to be represented [18]. However, archetype-based models tend to perform more poorly at a finer time resolution, such as in capturing the district's hourly load profile [18]. Whether existing buildings or hypothetical ones are being modeled, realistic hourly load profiles are key to the meaningful analysis of district thermal energy systems, due to the nonlinear nature of the performance curves of primary equipment such as chillers, boilers, and heat pumps. One factor contributing to the deficiency of many archetype models in predicting energy use at a short time resolution is a reliance on deterministic values of modeling parameters, which fail to capture the wide degree of variation in the actual values of those parameters, even among buildings with similar characteristics [19].

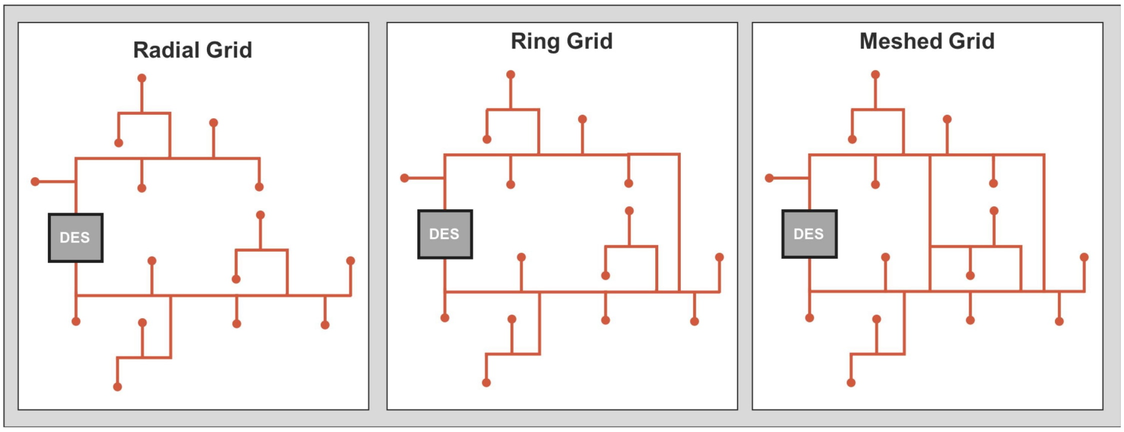

Figure 2: Grid topologies for district thermal energy systems, courtesy of [10]

Parameters related to occupant behavior, including schedules for occupancy and lighting and plug loads, have some of the highest levels of uncertainty and are also key drivers of energy use in residential buildings [19]. The work of [20] developed a methodology for Bayesian calibration of normative energy models in the context of large-scale retrofits, and used the Morris method for parameter screening. The authors identified lighting and plug load densities as highly influential parameters. In [21], a sensitivity analysis was performed for building heating and cooling energy end-uses specifically, considering occupancy and load densities, material properties, and design considerations such as window-to-wall ratio. The authors identified infiltration rate as being one of the most influential parameters. To address these sources of uncertainty, past studies have attached probability distributions to uncertain input parameters, and generated distributions of expected building energy use. This approach is also generally extensible to representing energy use of districts, with individual buildings being assigned parameter values through probability distributions.

1.4. Topology optimization

In this work, district energy system network topologies are represented using the mathematical concept of *undirected graphs*. An undirected graph consists of a set of vertices, or nodes, and a set of edges, which can be expressed as unordered pairs of nodes [22]. A *connected graph* is one in which there exists a path between each and every pair of nodes. The connectivity of a graph can be represented by an *adjacency matrix,* $\boldsymbol{A}$, in which an element $A_{i,j} = 1$ if there exists an edge between nodes i and j and 0 otherwise. In graph theory, a cycle is a path that starts and ends at the same node, and passes through at least three distinct nodes [22]. A connected graph without cycles is considered a spanning tree. A minimal spanning tree is the spanning tree with the least total edge length. Interpreted in the context of district energy system topologies, the minimal spanning tree represents the network that achieves the connectivity of a given set of buildings with the least infrastructure cost. In this study, the minimal spanning tree (MST) heuristic is evaluated to select the network by which a given set of buildings should be connected.

Topology optimization is particularly relevant in the context of 5GDHC systems. Such systems create the potential for buildings and industrial processes to act as “prosumers”, supplying or rejecting heat to the thermal network in a way that can offset the load on centralized primary equipment. As a result, more complex network topologies, such as ring and meshed configurations, are often implemented for systems of this type [10]. In the context of conventional district thermal energy systems, where heat and mass flow are typically uni-directional, radial networks are generally used, unless redundancy of supply is essential [10]. Fig. 2 shows a schematic of radial, ring, and meshed network topologies. Initial work by others suggests that ring and meshed networks can deliver benefits in energy- and exergy-efficiency under certain conditions. The work of [23] compared ring and radial networks for a 5GDHC system through a simulation study, and found that ring networks could incorporate distributed sources of waste heat more effectively. A simulation study by [24] compared two different configurations of 5GDHC systems. The authors found that a two-pipe system with bi-directional flow, similar to the one considered in this study, with a meshed network configuration, resulted in a greater exergetic efficiency than a single-pipe system with uni-directional flow. However, the costs associated with piping and trenching are a significant part of the overall life cycle cost of the district thermal energy system, as concluded by [25] and others. These potential trade-offs between initial capital cost and energy performance motivate the need for a topology optimization framework to guide decisionmaking.

Past studies addressing topology optimization for district thermal energy systems differ in terms of the range of topologies considered and whether connected loads were treated as boundary conditions, as well as in the nature of the thermal networks considered, and the fidelity of building load profiles. Topology optimization problems in this context have often been formulated as mixed-integer non-linear programs (MINLPs), and genetic algorithms have often been leveraged for solving the problem. Life cycle cost, accounting for operating energy as well as the annualized capital cost, has often been chosen as the objective function. In [25], an optimization problem was solved for the network topology (including location of the central plant) and pipe diameters to minimize life cycle cost for a low-temperature district heating network. The network topology was constrained to be a tree and a connected graph and the connection status of each building was taken as a boundary condition. Building loads were represented with an annual peak load, and a multiplier for each of eight periods dividing the year. The authors of [25] concluded that the spatial lay-out of the district considered, building heat loads, and pressure and temperature requirements for the network were key factors influencing the optimal topology. The authors of [26] performed a simultaneous optimization for sizing of a combined heat and power (CHP) plant and topology of the associated district heating network, with annual net profit as the objective function, accounting for initial capital investments and operating income from the sale of electricity and heat. Thus, the interactions between the network topology and operating energy were not directly reflected in the objective function. The analysis was performed for only one set of load conditions. With the constraint of at least one connected building, the connection status of other considered buildings was an optimization variable. The authors considered radial and ring, but not meshed, topologies. They applied theirmethodology to several study cases and concluded that the simultaneous optimization of the plant design and network topology resulted in increased profitability relative to separate optimizations due to the interactions between the thermal and electrical systems.

Other studies have considered more flexible thermal network configurations. The work of [27] sought to optimize the topology configuration, pipe diameter, and operating parameters of a district heating network for minimal life cycle cost. Operating parameters included supply and return temperatures for the network, and mass flow rates. Both parallel and series connections of buildings to the district network were considered, as well as the absence of a connection from a given building to the network. The primary application for series connections were buildings with lower temperature supply requirements [27]. The authors of [27] formulated the problem in three sub-problems as a mixed integer nonlinear program, a mixed integer linear program, and a nonlinear program and performed the analysis for steady-state conditions only. They considered several sample configurations of building locations and loads, and concluded that the optimal topology was highly context dependent, and not generalizable.

Other studies have considered objective functions other than economic cost, or multiple objectives. The work of [28] applied topology optimization to a district heating network, with an objective of robustness to fluctuations in minimum supply pressure head. In their work, pipe diameter (with a minimum value of zero, corresponding to the non-existence of the thermal connection) was the optimization variable, and meshed networks were considered. The authors applied a method of moving asymptotes approach to the optimization problem. The connection status of buildings to the network was treated as a boundary condition. The authors of [28] found that the network connectivity was much more influential on robustness than the sizing of pipes. The work of [29] considered multi-objective optimization (for life cycle costs and carbon emissions) for district-level heating and electrical energy systems. In [29], the optimization problem was divided into three sub-problems: selection of heating systems for each building (which could be tied to a district system, or independent), design of primary equipment (with energy storage included in the scope) and selection of efficiency measures at the building level, and operation of primary equipment and energy storage units. The authors of [29] used detailed building load models, formulated with resistor-capacitor (RC) networks. They considered various topology configurations, but not meshed networks. Their solution process was iterative among the three sub-problems. The authors of [29] concluded that, for the hypothetical district considered, distributed CHP and auxiliary heat generation was more cost-effective than a centralized CHP system. The work of [30] performed a multi-objective optimization for design and control of a low-temperature district heating network leveraging renewable thermal and waste heat sources. The consumption of imported primary energy, annualized costs, and carbon emissions were the considered objective functions. The optimization variables included the sizing and location of solar thermal collectors, seasonal thermal energy storage, and waste heat injection, as well as the diameters of network pipes, with a zero diameter corresponding to the absence of a pipe from the network. Individual building loads were aggregated to larger nodes representing neighborhoods, and the connection of these nodes to the network was treated as a boundary condition. The authors applied a master-slave approach to the joint design and control optimization. The authors of [30] concluded that their results for a study case were not readily generalizable to design guidelines, but supported the heuristic that thermal sources should be located close to large loads.

Other studies of topology optimization for district thermal energy systems have investigated the effects of the selection of the objective function. The work of [31] compared the outcomes of optimized design of a district heating and cooling network under two different objective functions: capital costs and life cycle cost, formulating the problem as a mixed-integer linear program. The authors effectively constrained the analysis to radial or ring topologies, and considered energy consumption associated with distribution pumping and heat losses, but treated the energy consumption at loads, and their connection status, as boundary conditions, and performed the analysis for a static load condition. In a study case, the authors identified differences between the topologies of the networks optimized under the two objective functions, due to differences in pumping energy and heat loss associated with the networks, further motivating the need for network topology optimization. The authors of [31] identify consideration of higher-fidelity load profiles, as well as greater flexibility in the network configuration, as areas for future work in the optimization of district thermal networks.

1.5. Novelty and contribution

Among past works addressing topology optimization for district thermal energy systems, some studies, such as [28], have addressed objective functions that are not influenced by energy consumption. Others, such as [25], [27], [30], [26], and [29] addressed objective functions influenced by energy consumption, but in the context of district heating networks only. This study introduces greater complexity by analyzing an advanced district thermal energy system, with an objective function influenced by energy consumption and investment and operating costs. Addressing the need identified by [31], ambient loops and low-temperature district heating networks create more interesting opportunities for optimization than high-temperature heating only networks, by introducing more potential topologies, and the potential for bidirectional thermal and mass flow. The larger effort to develop a topology optimization framework, of which this study is a part, presents a departure from past work because it considers both the questions of which subset of buildings to connect as well as how they should be connected, is flexible to a variety of potential topologies, and considers high-fidelity building load profiles. This effort extends the work of [10] and [32] by leveraging tools developed by those authors (specifically the 5GDHC Topology Analysis Tool and the Metamodeling Framework), to evaluate the minimal spanning tree heuristic for a larger use case, and test the hypothesis that the heuristic is effective in selecting the least-cost network.

An additional novelty of this contribution is the joint consideration of building- and district-level HVAC system energy performance, and the network topology optimization problem. Low-energy districts are an ideal case for the analysis of radiant hydronic HVAC systems, and comparisons with air-based systems. Existing literature, such as [16] and [33], has focused on comparisons of TABS and air-based systems at the building level. Prior work has not addressed district thermal energy systems serving multiple buildings with load profiles accounting for stochasticity of energy use. To test the hypothesis that radiant hydronic HVAC systems will save energy at the district level relative to air-based systems, a detailed comparison of the energy performance of two hypothetical districts is performed.

2. Methods

This study comprises two analyses, both of which evaluate the potential of advanced district thermal energy systems: the comparison of the energy performance of two HVAC system types at the urban district level, and the evaluation of a heuristic for topology optimization of district thermal networks.

2.1. Heating, ventilation, and air-conditioning (HVAC) system comparison

In this study, the energy performance of two hypothetical low-energy residential districts, one with air-based HVAC systems, and one with radiant hydronic HVAC systems, was compared. Both districts were served by district thermal energy systems. In both cases, to generate the district energy model, a representative building energy model was perturbed to reflect a larger number of buildings. The following steps were performed to carry out this analysis:

1. Adapt a prototype building model for each HVAC system type under consideration (air-based and radiant hydronic systems).
2. Perturb each base building model to generate ten building models for each district.
3. Perform energy simulations at the individual building level for the districts, with the building models controlled to achieve an equal level of thermal comfort. Generate heating and cooling load profiles for the district thermal energy systems.
4. Assemble energy models for the primary heating and cooling plant serving each district, using EnergyPlus components, and simulate with the load profiles generated in step 3.
5. Evaluate results based on load intensity and annual heating and cooling energy use intensities.
6. Derive general conclusions from the particular case study.

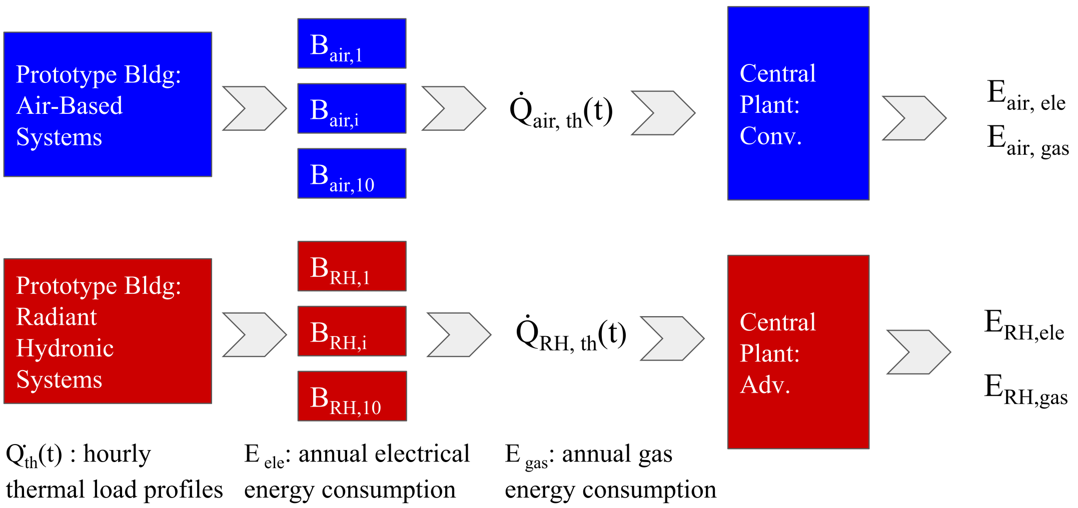

Figure 3: Analysis process performed for HVAC system comparison

The process for this analysis is also illustrated in Fig. 3. In Fig. 3, energy models representing air-based systems and the conventional central plant are shown in blue, and energy models representing radiant hydronic systems and the advanced central plant are shown in red.

Energy simulation for this analysis was performed using EnergyPlus v8.9 [34]. The analysis was performed using a typical meteorological year (TMY3) weather file for Denver, Colorado, a climate with both heating and cooling loads. Energy consumption results were analyzed in terms of both site energy and source energy, with source energy used as the ultimate basis for comparison. Site energy refers to the energy delivered to a site (in this case interpreted as a district). Source energy encompasses all the inputs required to generate the delivered energy, including losses in electricity generation, transmission, and distribution, and in natural gas distribution [35].

2.1.1. Base building energy models

The intention of this analysis was to isolate the effects of the difference in HVAC systems between the two districts. Thus, the building models for the two districts were identical, except for the HVAC system types. To represent a low-energy district, a base building model with a high-performance envelope and efficient HVAC systems (compliant with 2013 ASHRAE 90.1 [36]) was adapted from a prototype building model. The U.S. Department of Energy publishes prototype building energy models in EnergyPlus format, which are intended to represent the characteristics of typical commercial and multi-family residential buildings in the U.S. [37]. The multi-family prototype model, located in ASHRAE Climate Zone 5B and compliant with 2013 ASHRAE 90.1, was modified to create the base building energy models. The multi-family prototype building model represents a four-story building, of 3,130 m^2 in floor area, composed of residential units and a small office space on the ground floor. The construction is steel frame,

Table 1: Summary of base model envelope and load characteristics

Parameter	Value
Space allocation	
Residential area (%)	87%
Corridor area (%)	10%
Office area (%)	3%
Envelope properties	
Wall U-value($\frac{W}{m^2K}$)	0.31
Roof U-value($\frac{W}{m^2K}$)	0.17
Floor U-value($\frac{W}{m^2K}$)	0.24
Window U-value($\frac{W}{m^2K}$)	0.42
Window SHGC	0.40
Internal loads	
Occupant density ($\frac{person}{1000m^2}$)	25.0
Lighting power density ($\frac{W}{m^2}$)	14.0
Internal load density ($\frac{W}{m^2}$)	6.70

and the building has a window-to-wall ratio of 20%. Windows are double-pane with a low-emissivity coating. The prototype building model is configured with split systems with direct expansion cooling and natural gas heating to serve each thermal zone. Internal loads other than lighting in each residential unit include kitchen appliances, a washer and dryer, and miscellaneous plug loads, all of which are powered by electricity. Characteristics of the envelope and loads of the prototype building model, which are retained in the base building model, are summarized in Table 1.

The HVAC systems in the prototype building model were modified to generate the base building models for this study. For the district with air-based systems, the split systems were replaced with air handling units with hydronic coils, in order to allow integrating the building level systems with district thermal energy systems. Heating hot water from the district loop was supplied to these systems at 82°C, and chilled water was supplied at 7°C. The air-based systems were controlled to achieve neutral thermal comfort in the space, as reflected in the Fanger model (using the control object (Thermostat:ThermalComfort) in EnergyPlus).

For the district with radiant systems, the split systems were replaced with low-temperature, variable-flow, radiant hydronic heating and cooling systems, integrated in the floor slabs. Due to the large area available for heat transfer, heating hot water and chilled water were supplied at moderate temperatures. Heating hot water from the district loop was supplied to the radiant systems at 45°C and chilled water was supplied at 16°C. The flow rate of hot water or chilled water through the radiant hydronic coils was controlled based on operative temperature in the zone, consistent with the approach taken in [12]. A dedicated outdoor air system (DOAS) was added to the model to supply tempered ventilation air, at a constant volume. The DOAS units were each equipped with a direct-expansion (DX) cooling coil and a gas heating coil to temper the outside air. The radiant hydronic HVAC system model incorporated in EnergyPlus is documented in [38]. The work of [39] performed a validation of the EnergyPlus radiant hydronic system model in the context of an instrumented residential building with radiant systems, and found a good correspondence between predicted and experimental results for the energy consumption and thermal comfort parameters considered.

The DOAS units were equipped with a heat recovery ventilator (HRV), in the form of a run-around loop. A run-around loop avoids the risk of cross-contamination between supply and exhaust air from different residential units. Heat recovery ventilation is required by 2013 ASHRAE 90.1 for HVAC systems in ASHRAE Climate Zone 5B supplying 100% outdoor air, but not for systems supplying less than 50% outdoor air at full design flow rate, as is the case for the hydronic air handlers serving the buildings with air-based systems [36]. Thus, heat recovery ventilation was not modeled in the hydronic air handling units.

2.1.2. Perturbations of building energy models

To generate realistic heating and cooling load profiles for the district thermal energy system, characteristics of the base building model were perturbed in order to generate nine other sets of characteristics, which were then implemented in nine other versions of the base building energy model. The same sets of perturbations were used for both the district with air-based systems and the district with radiant systems. The following parameters were perturbed using probability distributions: window-to-wall ratio, internal load density, occupant density, and infiltration rate. These parameters were selected based on the uncertainty associated with them in a hypothetical building, and their influence on heating and cooling loads, determined through a literature review. Ranges for the parameter values were selected based on the literature, (as previously discussed, [19], [20], [21]), and existing guidelines for energy modeling of residential buildings. Schedules for occupancy and internal loads were also adjusted using probability distributions to select a duration by which to "expand" or "contract" the schedule, and to shift the schedule values. These schedules were adjusted in order to reflect the stochastic nature of occupant loads and occupant-driven energy use, both of which contribute to the temporal distribution of building heating and cooling loads [19]. Table 2 shows the ranges over which these parameters were perturbed, the distributions used, and references used to determine the ranges. The approach for shifting occupant and plug load schedules was developed by the authors.

Table 2: Parameter space for building model perturbations

Parameter	Dist. Type	Min.	Max.	Ref
Internal load density ($\frac{W}{m^2}$)	Triangular	6.7	16	[40]
Occupant density ($\frac{person}{1000m^2}$)	Triangular	17	50	[19] and [40]
Window-to-wall ratio (%)	Uniform	15	40	[40] and [41]
Infiltration rate($\frac{\frac{m^3}{s}}{m^2 \text{wall area}}$)	Triangular	0.2	2.0	[42]
Occupancy schedule shift (hours)	Triangular	-3.0	3.0	N.A.
Internal load schedule shift (hours)	Triangular	-3.0	3.0	N.A.

2.1.3. System comparison and thermal comfort

A meaningful comparison of energy performance must ensure that different HVAC system types are delivering the same degree of thermal comfort in a conditioned space. Thus, the two system types were controlled to achieve the same degree of thermal comfort, as closely as possible, reflected by the Fanger model, which is widely accepted for evaluating thermal comfort [43]. The predicted mean vote (PMV) for occupants in a space is a metric typically used to interpret the results from Fanger's model, with values ranging from -2 (very cold) to 2 (very warm), and a value of 0 corresponding to thermal neutrality. The modeling approach leveraged an option in EnergyPlus to control air-based systems to a thermal comfort setpoint. The radiant systems were controlled to the sequence of operative temperatures that previously resulted in the buildings with air-based systems. This approach resulted in a near-perfect alignment of PMV between corresponding buildings at each timestep and maintained PMV generally within the acceptable band of [-0.5, 0.5] overall. The analysis of thermal comfort serves to ensure that the same degree of service is being provided by the two HVAC system types considered, and thus that a direct comparison of their loads and energy performance is valid.

2.1.4. District thermal energy system models

The central plants serving the two districts were modeled with the same types of primary equipment, and the same network of distribution pumps and pipes. The primary equipment consisted of water-cooled centrifugal chillers, cooling towers, and hot water boilers. Both districts were configured with a primary and distributed secondary pumping arrangement, with variable-speed pumps.

Characteristics of the chillers and boilers in each plant are shown in Tables 3 and 4. Note that the COP value listed is for the chiller alone, and not the chilled water plant as a whole.

Both central plant models were configured with water-side economizers, which use heat exchangers between the

Table 3: Summary of chiller characteristics

Unit	Cooling Capacity	Chiller Rated COP $(\frac{W}{W})$	Quantity
Shoulder season chiller	130	5.9	1
Peak load chiller	470	8.2	3

Table 4: Summary of boiler characteristics

Unit	Heating Capacity(kW)	Nominal Efficiency(%)	Quantity
Condensing boiler	200 to 2,900	89%	4
Non-condensing boiler	200 to 2,900	80%	4

condenser water and chilled water loops, to allow heat to be rejected directly from the chilled water return to the condenser water, when the condenser water is sufficiently cool. Chiller characteristics, including performance curves and reference efficiency and capacity values, were obtained from datasets available in EnergyPlus, which represent chillers that are or have been produced by manufacturers [34]. The rated COP values are compliant with the standards for full-load and integrated part-load efficiency in 2013 ASHRAE 90.1 for equipment manufactured through 2015 [36].

The central plant serving the low-exergy systems is configured with condensing heating hot water boilers. The central plant serving the air-based systems is configured with non-condensing heating hot water boilers. The nominal efficiency values of the boilers are compliant with 2013 ASHRAE 90.1 [36]. The higher return temperatures in the heating hot water loop serving the conventional systems (observed to be 60°C under typical conditions) are too warm to achieve condensing in a condensing boiler [44]. After generating a load profile based on the ten buildings modeled in each district, the thermal and electrical load profiles of each district were multiplied by a factor of four, to better align the cooling load with the capacities of water-cooled chillers available on the market. Thus, each district model effectively represented forty buildings.

2.2. *Evaluation of minimal spanning tree heuristic*

It is hypothesized that topology optimization will enhance the cost-effectiveness of advanced district thermal energy systems, such as the low-exergy systems analyzed in this study. The minimal spanning tree heuristic for the topology optimization problem was evaluated for a prototypical urban district, through a search of all spanning tree networks. The cost function implemented in the topology optimization problem corresponds to the life cycle cost, evaluated over a twenty-year time horizon, with a discount rate of 3%, of piping infrastructure for the 5GDHC system, as well as the energy required to meet the HVAC loads of all buildings in the district, whether or not they are served by the 5GDHC system. The cost function accounts for projected escalations in electricity and natural gas rates, and for a potential future price on carbon dioxide (CO_2) emissions, based on a scenario outlined by the U.S. National Institute for Standards and Technology [45], as well as projected future declines in the carbon intensity of electricity. The formulation of the objective function leverages uniform present value (UPV) factors for the selected discount rate and time horizon, which represent a ratio of the life cycle cost to the annual cost. UPV factors are obtained from [45] for the operating cost streams (electricity, gas, and carbon) and also reflect the projected escalations in the costs of these quantities over the project lifetime. The analysis is performed based on an application of the energy consumption over a simulated year to all years of the time horizon. This formulation of the cost function is consistent with that implemented by [10]. The cost function for the topology optimization problem is formulated as shown in Eqn. 1.

$$\begin{aligned} \min_{\mathbf{A}} C_{pipes} + C_{elec} UPV_{elec}(E_{de} + \sum_{i=1}^{n} E_{be,i}) + C_{gas} UPV_{gas} \sum_{j=1}^{n} E_{bg,j} \\ + \sum_{t=1}^{20} m_{CO2}(t) C_{CO2}(t) UPV_{CO2} \end{aligned} \tag{1}$$

subject to:

(1): If there exists a pipe directly thermally connecting building i and building j, $A_{i,j} = 1$. Otherwise, $A_{i,j} = 0$.

(2): If building i is served by the district thermal energy system, there exists a path from the central plant to node i.

where $\mathbf{A}$ is the adjacency matrix describing the thermal network, C_{pipes} is the cost of pipes and trenching, C_{elec} is the electricity cost per unit of consumption, C_{gas} is the natural gas cost per unit of consumption, $E_{be,i}$ is the annual electric consumption for HVAC at building i, E_{de} is the annual electric consumption for district energy systems, including primary equipment and distribution pumps, $E_{bg,j}$ is the annual natural gas consumption for HVAC at building j, UPV_{elec} is the uniform present value factor for electricity, UPV_{gas} is the uniform present value factor for natural gas, $m_{CO2}(t)$ is the annual carbon emissions in a given year, $C_{CO2}(t)$ is the cost associated with carbon emissions in a given year, and UPV_{CO2} is the uniform present value factor associated with carbon pricing. Note that the time-dependence of carbon emissions and their associated cost is due to the projected future declines in carbon intensity of electric generation, and the projection of an escalating carbon tax.

Note that with n buildings, in addition to a central plant, the graph representing the network has $n+1$ nodes. Due to the complex interactions among building loads in the district energy system context, as well as the equations governing

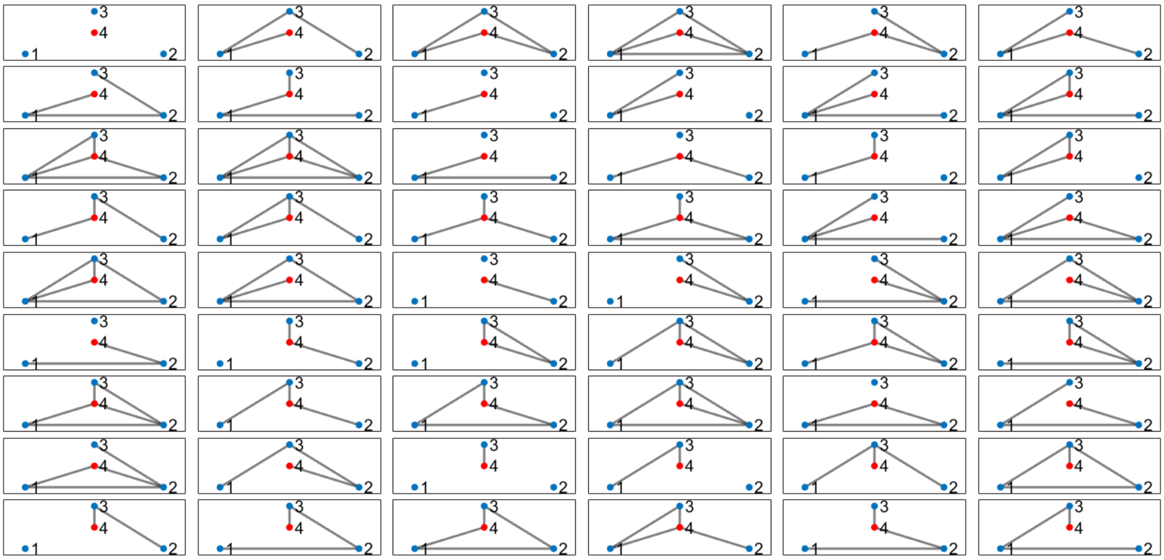

Figure 4: Topology optimization search space for district consisting of three buildings and DES plant

energy consumption by pumps, and heat losses through the pipes, the energy consumption terms in this function are nonlinear. The functions used to evaluate building thermal loads, which are discussed in a following sub-section, are non-convex. Thus, the problem formulated in Eqn. 1 is non-convex, due to the binary nature of the elements of the adjacency matrix, and the non-convex functions for energy consumption.

The number of potential solutions to the topology optimization problem formulated in Eqn. 1 is a function of the number of possible subsets of buildings in the considered district, and the number of ways in which a given subset can be thermally connected. Specifically, the number of potential solutions is equal to the product of the number of ways to select a subset of buildings of a given cardinality and the number of ways in which that subset can be connected, summed over the number of buildings in the district. There is one additional solution corresponding to the case in which no buildings are connected to the network. Fig. 4 explores all fifty-four possible solutions to the topology optimization problem for a district consisting of three buildings (shown with blue nodes) and a district energy plant (shown with a red node).

As illustrated in Fig. 4, the size of the search space quickly expands with an increasing number of buildings. This makes an exhaustive search impractical. A means of addressing this is dividing the analysis of the problem into two steps, first addressing the question of "which subset of buildings should optimally be connected to the district energy system," followed by, "given the optimal subset of buildings, what is the best means by which to connect them?" It was hypothesized that a minimal spanning tree may be a suitable heuristic for connecting a given subset of buildings, addressing the second sub-problem. A minimal spanning tree minimizes the piping and trenching costs relative to

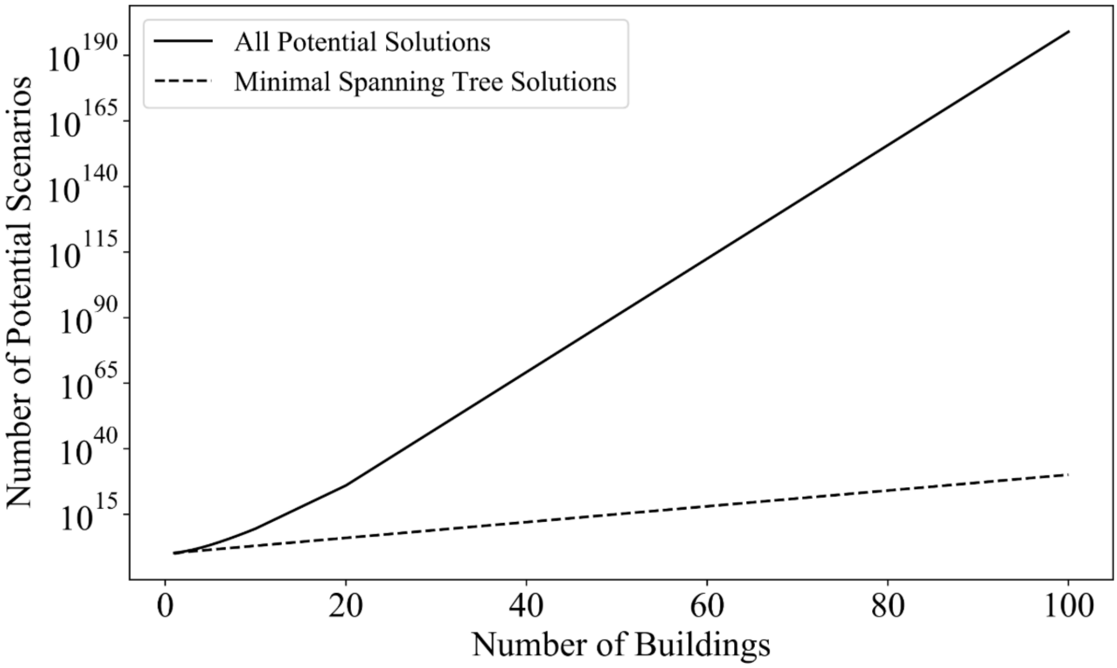

Figure 5: Comparison of the sizes of the full search space and search space of minimal spanning trees

other potential networks. The costs associated with piping and trenching are a significant part of the overall life cycle cost of the district thermal energy system, as concluded by [25] and others. The use of the minimal spanning tree heuristic would significantly reduce the size of the search space for the topology optimization problem as a whole. As there exists a unique minimal spanning tree for each subset of buildings, the use of this heuristic reduces the search space to the number of distinct combinations of buildings, which is equal to 2^n for a set of n buildings, including the null set. Fig. 5 compares the number of possible minimal spanning trees to the size of the solution set as a whole as a function of the number of buildings considered. (Note that the y-axis in Fig. 5 is non-linear.) The number of minimal spanning trees also becomes intractable for districts of increasing size. Additional means of reducing the size of the potential solution space for larger prototypical districts are an area of future work in development of the topology optimization framework.

In this study, all possible spanning tree networks that could serve a district consisting of four buildings and a central plant were analyzed, constituting 212 different cases. A Modelica energy model of the 5GDHC system was used to evaluate the energy consumption terms in the cost function. Modelica is an object-oriented, equation-based language for modeling physical systems [46]. The underlying energy model was assembled and documented in [10] as the 5GDHC Topology Analysis Tool. The model was validated by the authors of [10] using data from a laboratory test bed operated under the FlexyNets Project. FlexyNets is a Horizon 2020 European Project which seeks to develop and

Table 5: Building characteristics, evaluation of MST heuristic

Building Type	Floor Area(m^2)	Baseline HVAC System Type
Retail	2,294	Packaged units with DX cooling and gas heating
Office	512	Air source heat pumps with supplemental gas heating coils

deploy fifth-generation district heating and cooling networks [47]. As part of the validation, model parameter values were adapted to reflect those of the FlexyNets test bed, and the model was initialized to a consistent set of conditions. Fluid temperatures calculated by the model at specific points in the thermal network were compared to those measured in the FlexyNets test bed, and a satisfactory correspondence was found [48]. The load side of the energy model was expanded in this work to represent a prototypical urban district consisting of three identical office buildings, and one larger retail building. Based on the work of [13] and [10], it is expected that increased thermal load diversity will enhance the viability of advanced district thermal energy systems. Consistent with the approach taken by [10], in the 5GDHC energy model, building thermal load profiles were represented with data-driven metamodels, generated with the Metamodeling Framework developed in [32]. The Metamodeling Framework has been demonstrated to represent building thermal load profiles accurately, and improves the efficiency of the 5GDHC model simulation, compared with the use of full-order, physics-based models to represent building loads. In the framework developed by [32], metamodels of building thermal load profiles are trained based on a dataset developed using the U.S. DOE prototype building energy models. The Metamodeling Framework offers several model types, and random forest models were used in this study. Two thermal load profiles are developed for each building: one for the case in which the building is tied to the 5GDHC system, and one for the case in which the building is served by independent systems. Separate training data sets are used to generate metamodels for the connected and independent cases. Characteristics of the prototypical buildings used to generate load profiles using the Metamodeling Framework are shown in Table 5. For the independent case, the DOE prototype building models, in their current form, are used, with a parameter sweep, to generate training data. For the connected case, the models are modified to use water-source heat pumps for space conditioning. Analysis was performed for the location of Golden, Colorado.

In this analysis, natural gas and electricity rates obtained from the U.S. Energy Information Administration for Colorado in 2017 [49], and unit costs for pipes and trenching ($500/meter), as documented in [48] were used. The twenty-year time horizon used in the analysis is consistent with that used in [48] for evaluation of a 5GDHC system. For purposes of calculating pipe lengths, and for visual reference, the four hypothetical buildings and a district energy system (DES) central plant were located on a block near the intersection of 13th Street and Washington Avenue in Golden, Colorado. A visualization of the GeoJSON data used to plot the building and DES locations is shown in

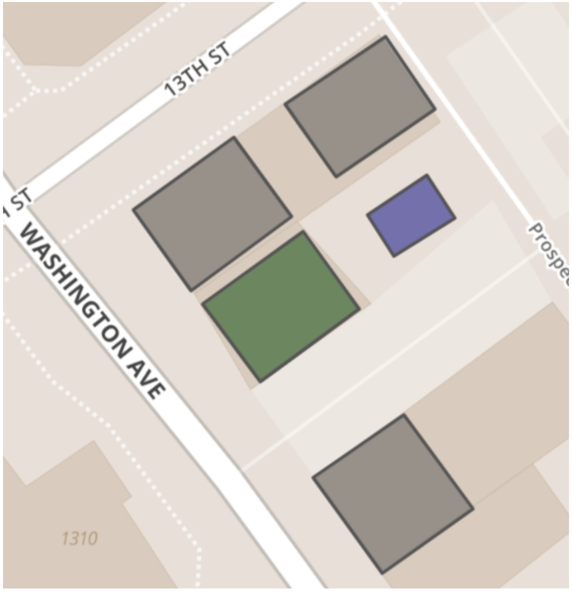

Figure 6: Visualization of building locations in hypothetical district (courtesy of GeoJSON.io)

Fig. 6. In the analysis, this data was used only for calculating pipe lengths. In Fig. 6, the office buildings are shown in brown, the central plant in blue, and the retail building in green. The relative sizes of the representational buildings shown are not to scale.

3. Results

Results from the HVAC system comparison and the evaluation of the minimal spanning tree heuristic for the topology optimization problem are discussed in the following sub-sections.

3.1. Heating, ventilation, and air-conditioning system comparison

As part of the HVAC system comparison, thermal comfort, HVAC system performance, and HVAC energy performance were analyzed. Results regarding HVAC system performance at the hydronic loop level and energy performance are presented in this work. Results regarding thermal comfort and zone-level HVAC system performance are presented in [50]. HVAC system performance at the hydronic loop level is quantified using metrics discussed by [16]. For both heating and cooling, cumulative distributions of heat added or extracted, respectively, at the hydronic loop level are shown normalized by building floor area, and disaggregated by the system component. Cumulative distributions of delivered cooling at the hydronic loop level for the base building are shown in Fig. 7 for air-based systems, and Fig. 8 for radiant systems. These values represent the cooling delivered by the cooling coil in the air handling unit for the air-based systems, and the sum of the cooling delivered by the DX coils in the DOAS units and

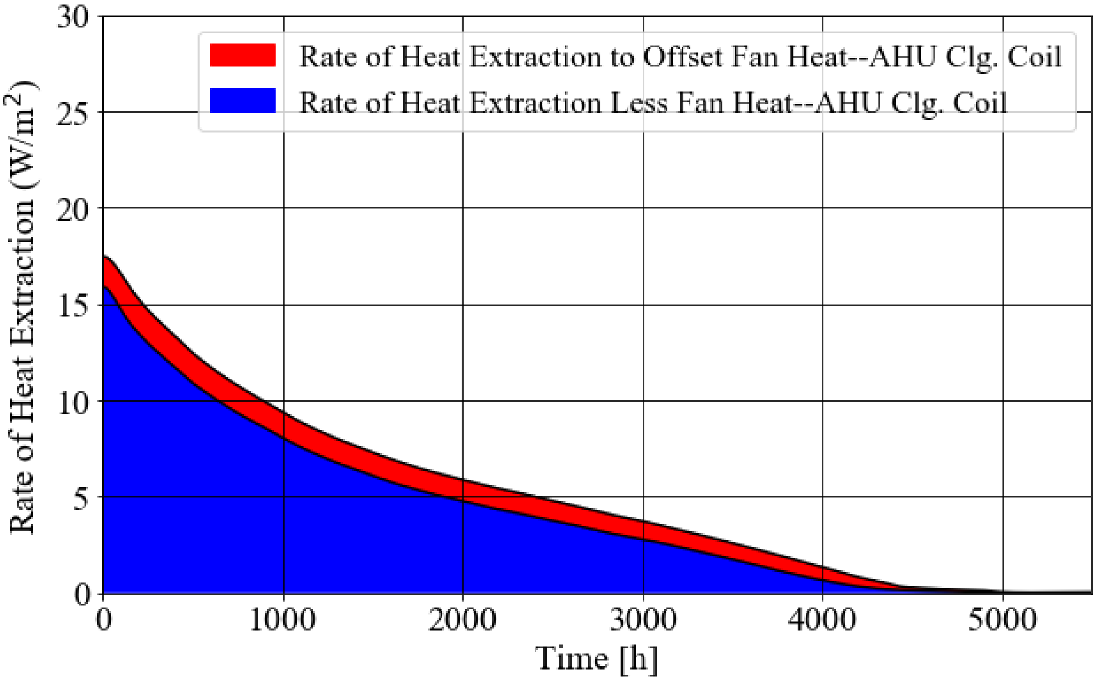

Figure 7: Cumulative distribution of cooling load at hydronic loop level, air-based systems

the zone radiant hydronic cooling systems for the radiant systems. Note that these values do not represent electrical power input in the case of the DX coils. The disaggregation of the delivered cooling associated with offsetting fan heat is shown for the air-based systems. Due to the lower installed fan power, the cooling load on the DX coil to offset fan heat is negligible for the radiant systems. The radiant systems experience a higher peak cooling load at the hydronic loop level (by 44%) than the air-based systems, which can be attributed to the more immediate conversion of long-wave and short-wave radiation into cooling loads. The ratio between the peak loads on the hydronic loop for the radiant and air-based systems is within the range found by [16]. The latent load constitutes a negligible portion of the total cooling load in both buildings, and thus a disaggregation of sensible and latent loads is not shown on these plots. [1]

As shown in Fig. 7 and Fig. 8, a non-negligible cooling load is present at the hydronic loop level in the building with air-based systems for significantly more time of the year than in the building with radiant systems. This difference is partially explained by the cooling load imposed by offsetting fan heat. Additionally, in the buildings with radiant systems, untempered ventilation supply air offsets a portion of the cooling load. The DOAS supply air is not tempered

[1]The 0.4% design wet bulb temperature for this location (Denver, Colorado, in ASHRAE Climate Zone 5B) is 18.5°C, with a mean coincident dry bulb of 27.4°C. That combination of wet and dry bulb temperatures corresponds to a relative humidity of 42.8%. The 0.4% design dry bulb temperature for this location is 32.9°C, with a mean coincident wetbulb of 15.9°C. That combination of wet and dry bulb temperatures corresponds to a relative humidity of 13.9% [51].

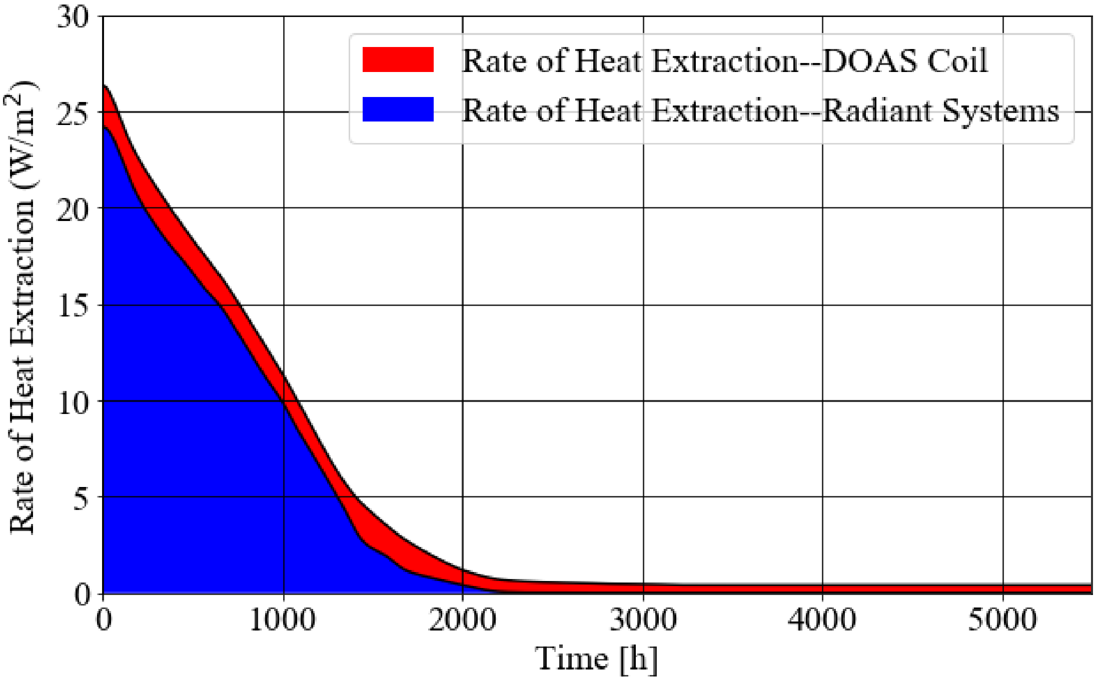

Figure 8: Cumulative distribution of delivered cooling at hydronic loop level, radiant systems

when outdoor air temperatures are between 12.8°C and 23.9°C. The ventilation supply air provides cooling, or creates a heating load, throughout the year, as the DOAS supply temperature is consistently below the zone air temperatures. During mild outside conditions, the DOAS effectively provides cooling through air-side economizing, though the outdoor air volume remains fixed. The cumulative annual thermal cooling loads of the two districts are similar. Due to the warm air temperatures in the buildings with radiant hydronic systems when the building is in cooling mode, the benefits of the heat recovery ventilator in cooling mode are minimal.

Plots of delivered heating intensities, at the hydronic loop level, are shown in Fig. 9 for the air-based systems and Fig. 10 for the radiant systems. These values represent the heating delivered by the heating coil in the air handling unit for the air-based systems, and the sum of the heating delivered by the heat recovery ventilator and the zone radiant hydronic heating systems for the radiant systems. Due to the presence of the HRV, the heating load on the gas coil in the DOAS units is minimal and is not shown on this plot. Note that the heating supplied by the heat recovery ventilator is not associated with additional energy use, but it is shown here for completeness in representing the thermal loads observed with both system types. The contribution of fan heat transferred to the supply air when the building is in heating mode ("useful" fan heat) is also shown for the air-based systems. Useful fan heat is negligible for the radiant systems, due to the lower airflows, and the presence of the HRV. The annual heating loads, also accounting for the effects of useful fan heat and heating delivered by the HRV, are similar between the two system types. The similarity

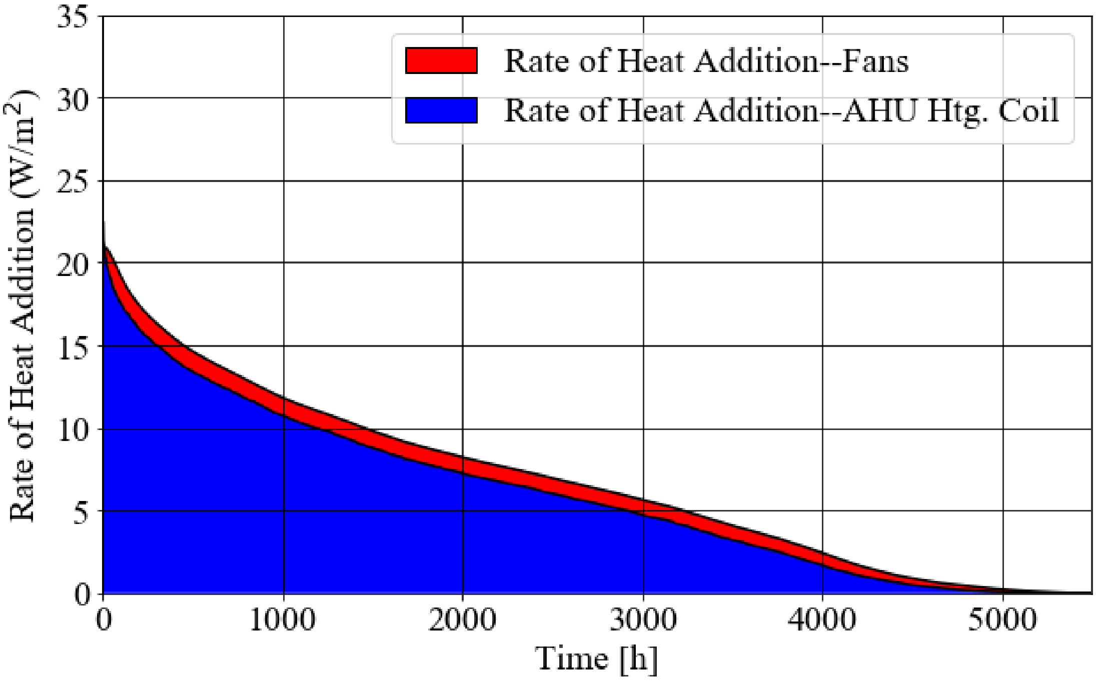

Figure 9: Cumulative distribution of delivered heating at hydronic loop level, air-based systems

in cumulative annual loads is expected in heating mode, due to the identical nature of the two buildings, expect for the HVAC systems. This result enhances confidence that the two systems are delivering the same service annually, and thus can be fairly compared on the basis of energy performance.

3.2. Energy performance comparison

The detailed analysis of loads at the hydronic loop level for the two system types provides insight into the expected energy performance comparison. Specifically, the similarity in cumulative annual heating and cooling loads between the two system types suggests that sources of distinction in their energy performance will relate to the presence of the HRV, the operating conditions of central plant equipment, and distribution equipment such as pumps and fans. The dry climate in the location analyzed in this study (Denver, Colorado in ASHRAE Climate Zone 5B) creates ample potential for water-side economizing. Due to the higher chilled water supply temperatures, water-side economizing can meet 53% of the chilled water load in the low-exergy district, compared with only 10% in the conventional district. The effects of water-side economizing are reflected in the ultimate energy use intensity of the chilled water plants. Energy use intensity of the two chilled water plants was compared with a metric including energy use associated with the chillers, cooling towers, and chilled water and condenser water pumps, and all cooling load delivered (including through water-side economizing). Performance metrics for the two chilled water plants, with and without

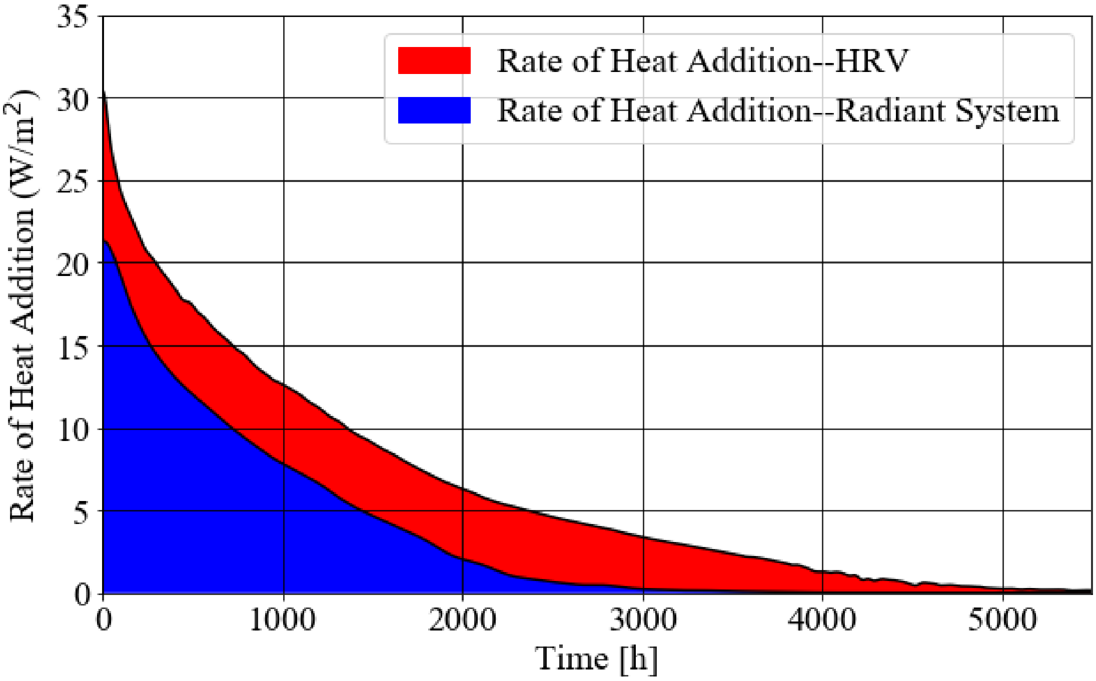

Figure 10: Cumulative distribution of delivered heating at hydronic loop level, radiant systems

the integration of water-side economizing, are shown in Table 6. As shown in Table 6, the higher chilled water supply temperatures in the low-exergy plant improve the chillers' efficiency, and the use of water-side economizing significantly improves energy performance for the low-exergy plant. Water-side economizing was implemented in both plants and is reflected in the analysis of their energy performance. The performance of the plants without water-side economizing ("base") is shown for reference.

As shown by the cumulative distributions of annual heating load in Fig. 9 and Fig. 10, due to the presence of heat recovery ventilation, the load on the district heating loop and gas heating coils serving the low-exergy systems is significantly lower than that on the conventional district heating loop. The annual requirement for active heating (excluding the heat recovered through the HRV) by the low-exergy district is 53% of that of the conventional district.

Fig. 11 shows a comparison of the disaggregated site HVAC energy use intensity at the district level for the two districts, calculated as the ratio of the total HVAC energy consumption in each modeled district to the total building floor area. Note that the floor area value is the same for the two modeled districts. The total site HVAC energy use intensity for the district with low-exergy systems is 51% lower than that of the district with conventional systems. Fig. 12 shows a comparison of the source HVAC energy use intensity at the district level for the two districts, with the end uses again disaggregated. The total source HVAC energy use intensity for the district with low-exergy systems is 49% lower than that of the district with conventional systems. The difference in the proportions of the two districts

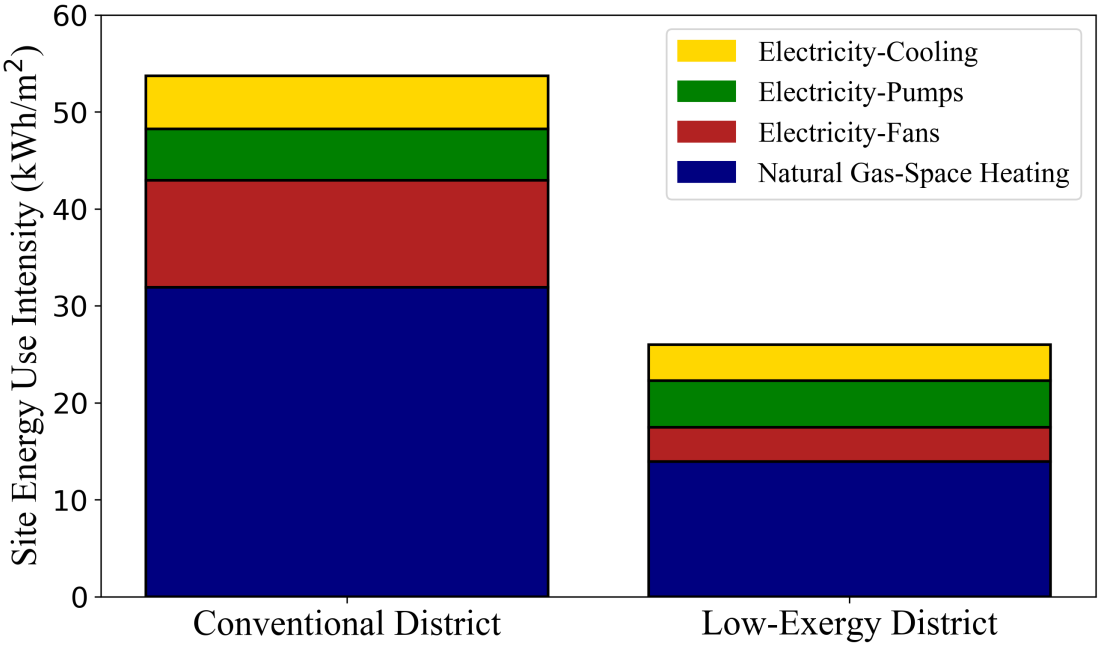

Figure 11: Comparison of site HVAC energy use intensity at the district level

in terms of site and source energy use intensity is a result of the fact that the energy use savings of the low-exergy district is largely driven by the gas energy savings associated with the HRV, which has a lower source-to-site ratio than electricity does.

Table 6: Summary of chilled water plant performance metrics

District	**Full Load Chiller Power** ($\frac{kW}{ton}$)	**CHW Plant Power (Base)** ($\frac{kW}{ton}$)	**CHW Plant Power(WSE)** ($\frac{kW}{ton}$)
Low-Exergy	0.33 and 0.43	0.62	0.44
Conventional	0.33 and 0.43	0.83	0.78

3.3. Evaluation of minimal spanning tree heuristic

The objective function as shown in Eqn. 1 was evaluated for all possible spanning tree networks for the prototypical district consisting of three office buildings, one retail building, and a DES central plant. Fig. 13 shows the life cycle cost as a function of total piping length for all 211 spanning trees that involve a connection to the DES, with color-coding corresponding to the number of buildings served by the DES. Note that the “null case”, in which all buildings have independent systems, is not shown here for compactness, but has the least life cycle cost of all potential solutions considered, a value of \$188,000. As shown in Fig. 13, when grouped by ascending life cycle cost, the potential

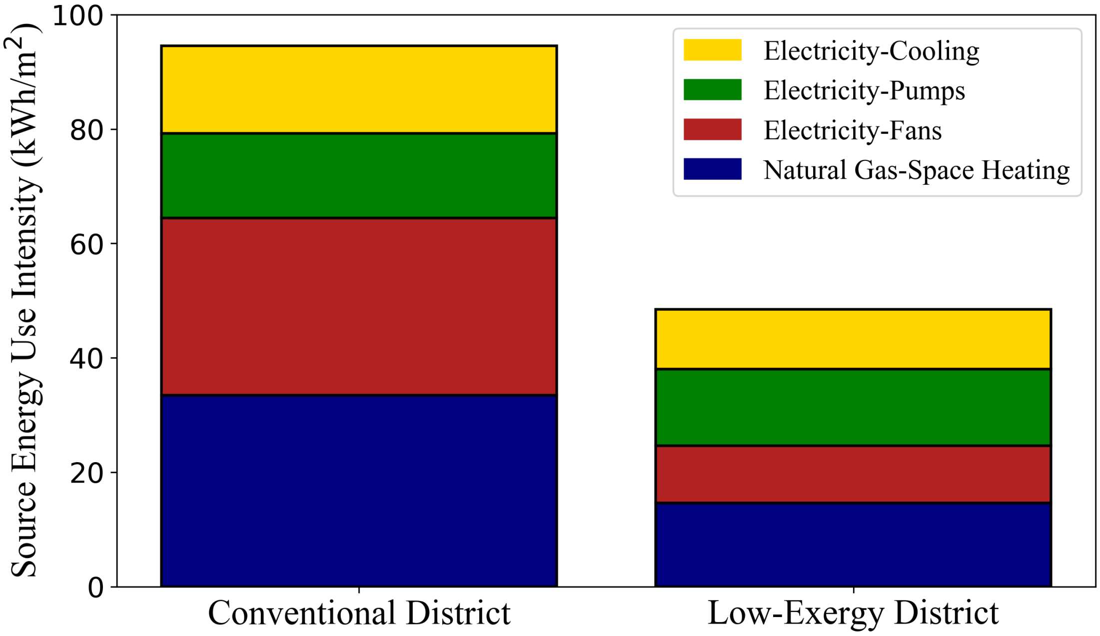

Figure 12: Comparison of source HVAC energy use intensity at the district level

solutions involving a connection of one, two, or three buildings are divided into two bands, based on whether or not the retail building is included in the network. The large step increase in life cycle cost between the two bands corresponds to the addition of the retail building to the network. The primary factor contributing to the bifurcation is the large heating load of the retail building in comparison with the office buildings, which are smaller in floor area and have significantly lower ventilation requirements. (The peak heating thermal load of the retail building is 115,000 W, compared with 15,000 W for the office building, and the annual heating energy consumption of independent systems is also correspondingly higher.) Given the prevailing electricity and natural gas rates for the location considered, it is much more costly to serve this large heating load with electricity as opposed to gas. The significant influence of the particular combination of connected loads on the system's life cycle cost performance is consistent with the results of [13]. As shown in Fig. 13, within each of the two bands of the solution space, the life cycle cost increases as a function of total pipe length. Of the potential spanning tree topology solutions for the prototypical district considered, infrastructure costs ranged from 2% to 28% of the overall life cycle cost, with the balance attributable to energy costs. Note that this fraction is expected to be higher for non-spanning tree networks, due to the greater length of piping used to connect a given subset of buildings.

From an analysis of the results of the spanning tree search, it is confirmed that, among spanning trees for this prototypical district, the minimal spanning tree network always results in the least life cycle cost for any given combination of buildings (in this case, subsets of two or three buildings, or the full four-building district). This result

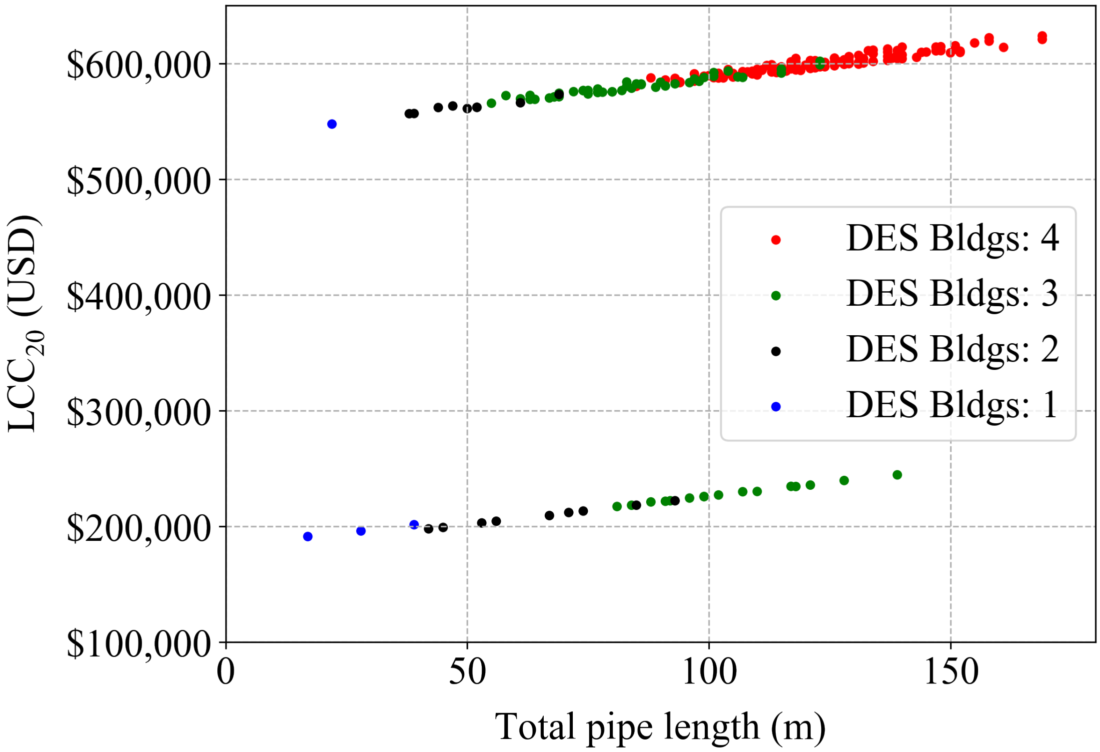

Figure 13: Life cycle cost and pipe length for spanning tree topology scenarios

is expected, as the non-minimal spanning trees result in higher pipe investment costs, without any expected benefits in thermal performance. This result is consistent with the results of [10], who validated the minimal spanning tree heuristic for a district of three identical buildings with an exhaustive search.

4. Discussion

The low internal load intensity of the hypothetical residential buildings studied in this analysis enabled the use of radiant hydronic systems, coupled with heat recovery ventilation, to meet almost the entirety of the heating and cooling loads, with minimal contribution from the air system. A building type with higher load intensities or located in a climate with higher latent loads from outdoor air would likely require more supplemental cooling from air-side systems, which would undermine the benefits of the low-exergy primary systems. The detailed analysis of system loads and the validation of the load intensity comparison results with those of [16] provide confidence in the results of the energy use comparison. The HVAC energy savings associated with the low-exergy district are driven by the use of heat recovery ventilation, and the lower energy intensity of the primary plant equipment serving the low-exergy systems. The lower energy intensity of the primary plant equipment is attributable to the higher nominal efficiency of the condensing boiler and its operating efficiency at a high loop temperature differential, more efficient operation of the chillers at the warmer chilled water supply temperatures, and increased potential for water-side economizing. The detailed analysis of loads at the individual building level in combination with analysis of a prototypical district represents a point of departure from previous studies. This analysis highlights the benefits of 5GDHC systems, for which topology optimization can facilitate cost-effective adoption.

Solving the topology optimization problem will require the use of non-convex optimization approaches, which are computationally intensive and can produce multiple solutions. In the future, as part of the development of the topology optimization framework, the minimal spanning tree heuristic will be evaluated with a full exhaustive search for a larger prototypical district with greater thermal load diversity . The prototypical four-building urban district for which the spanning tree search was performed demonstrated the potential of the minimal spanning tree heuristic, but did not offer sufficient thermal load diversity to reveal life cycle cost savings from a 5GDHC system, relative to independent building-level systems. In the full exhaustive search analysis, a sensitivity analysis to utility rates and to the investment costs associated with the district energy system will be performed. Based on the work of [10] and [13], it is expected that a prototypical district with a greater degree of thermal load diversity will be more likely to demonstrate life cycle cost benefits from 5GDHC systems, and from meshed networks specifically, and thus such a case will providean evaluation of the minimal spanning tree heuristic under the most relevant, and challenging, conditions. If the heuristic is demonstrated to be valid in a more complex case, it will be implemented as part of the framework. A black-box optimization algorithm that can use the Modelica simulation as a function evaluator, such as particle-swarm optimization [52], will be implemented to address the first part of the topology optimization problem, regarding the selection of a subset of buildings to connect to the district thermal energy system. [10] The implementation of the minimal spanning tree heuristic in the framework will enable topology optimization of 5GDHC networks without constraints on the connection status of individual buildings, providing a much more flexible approach than the current state-of-the-art, and opportunities to investigate complex interactions among building loads in a 5GDHC system.

5. Conclusions

The results of the HVAC system comparison demonstrate the potential of advanced district thermal energy systems to achieve deep energy savings. For the prototypical urban residential district considered, radiant hydronic HVAC systems mated with low-exergy district thermal energy systems achieved a source energy use intensity that was 49% lower than that of air-based HVAC systems and conventional district thermal energy systems. However, the high infrastructure costs and large solution space for potential network configurations hinder the adoption of advanced district thermal energy systems. The topology optimization framework proposed by the authors seeks to address those obstacles.

This study leveraged tools developed by [10] and [32] to evaluate a topology optimization heuristic for a four-building district, which demonstrated that the minimal spanning tree network was the most cost-effective means, among spanning trees, to connect a given subset of buildings through a 5GDHC system. This provides validation of the efficacy of the minimal spanning tree heuristic. The use of the minimal spanning tree heuristic significantly reduces the size of the solution space, and thus the computational complexity, of the topology optimization problem. In the future, this heuristic may be adopted by the proposed topology optimization framework. This study illustrated the promise for topology optimization to facilitate the adoption of advanced district thermal energy systems, which offer significant potential energy savings.

6. Acknowledgements

This work was authored in part by the National Renewable Energy Laboratory, operated by Alliance for Sustainable Energy, LLC, for the U.S. Department of Energy (DOE) under Contract No. DE-AC36-08GO28308. Funding provided by the Building Technologies Office and the Advanced Manufacturing Office. The U.S. Government retains and the publisher, by accepting the article for publication, acknowledges that the U.S. Government retains a nonexclusive, paid-up, irrevocable, worldwide license to publish or reproduce the published form of this work, or allow others to do so, for U.S. Government purposes. The assistance of Mr. Nicholas Long of the National Renewable Energy Laboratory, author of [32], in generating building load profiles using the metamodeling framework is gratefully acknowledged.

7. Nomenclature

Acronyms

5GDHC
: fifth-generation district heating and cooling

COP
: coefficient of performance

DOAS
: dedicated outdoor air system

DES
: district energy system

DX
: direct expansion

HRV
: heat recovery ventilator

HVAC
: heating, ventilation, and air-conditioning

MST
: minimal spanning tree

PMV
: predicted mean vote

RC
: resistor-capacitor

ROM
: reduced order model

TMY3
: latest collection of typical meteorological year data

Chemical symbols

CO_2

carbon dioxide

Variables

A

adjacency matrix describing the thermal network

C_{pipes}

cost of pipes and trenching

C_{elec}

electricity cost, as a rate per unit of consumption

C_{gas}

natural gas cost, as a rate per unit of consumption

$E_{be,i}$

annual electric consumption for HVAC at building

E_{de}

annual electric consumption for district energy systems, including primary equipment and distribution pumps

$E_{bg,j}$

annual natural gas consumption for HVAC at building *j*

UPV_{elec}

uniform present value factor for electricity, accounting for projected escalation in rates

UPV_{gas}

uniform present value factor for natural gas, accounting for projected escalation in rates

$m_{CO2}(t)$

annual CO_2 emissions, accounting for projections of reduced carbon intensity of electricity

$C_{CO2}(t)$

cost associated with CO_2 emissions in a given year, per projections under a scenario by NIST

UPV_{CO2}

uniform present value factor associated with carbon pricing

References

[1] T. T. Mai, P. Jadun, J. S. Logan, C. A. McMillan, M. Muratori, D. C. Steinberg, L. J. Vimmerstedt, B. Haley, R. Jones, B. Nelson, Electrification Futures Study: Scenarios of Electric Technology Adoption and Power Consumption for the United States, Nrel/Tp-6a20-71500 (2018). URL: https://www.nrel.gov/docs/fy18osti/71500.pdf. doi:10.2172/1459351. arXiv:1308.1667.

[2] European Commission, An EU strategy on heating and cooling 2016, Journal of Chemical Information and Modeling 53 (2016) 1689–1699. doi:10.1017/CBO9781107415324.004. arXiv:arXiv:1011.1669v3.

[3] H. Lund, P. A. Ostergaard, M. Chang, S. Werner, S. Svendsen, P. Sorknæs, J. E. Thorsen, F. Hvelplund, B. O. G. Mortensen, B. V. Mathiesen, C. Bojesen, N. Duic, X. Zhang, B. Möller, The status of 4th generation district heating: Research and results, Energy 164 (2018) 147–159. URL: https://www.sciencedirect.com/science/article/pii/S0360544218317420. doi:10.1016/J.ENERGY.2018.08.206.

[4] H. Lund, S. Werner, R. Wiltshire, S. Svendsen, J. E. Thorsen, F. Hvelplund, B. V. Mathiesen, 4th Generation District Heating (4GDH). Integrating smart thermal grids into future sustainable energy systems., Energy 68 (2014) 1–11. URL: https://www.tandfonline.com/doi/full/10.1080/23744731.2017.1366184. doi:10.1016/j.energy.2014.02.089.

[5] C. Carmichael, V. Olgyay, Managing Deep Energy Retrofits, 2012. URL: https://rmi.org/wp-content/uploads/2017/04/RetroFit_Depot_Managing_Guide_1.1.pdf.

[6] B. Polly, C. Kutscher, D. Macumber, M. Schott, From Zero Energy Buildings to Zero Energy Districts, in: 2016 ACEEE Summer Study on Energy Efficiency in Buildings, Asilomar, CA, 2016, pp. 1–16.

[7] D. Connolly, H. Lund, B. V. Mathiesen, S. Werner, B. Möller, U. Persson, T. Boermans, D. Trier, P. A. Østergaard, S. Nielsen, Heat roadmap Europe: Combining district heating with heat savings to decarbonise the EU energy system, Energy Policy 65 (2014) 475–489. URL: http://dx.doi.org/10.1016/j.enpol.2013.10.035. doi:10.1016/j.enpol.2013.10.035.

[8] H. Lund, N. Duic, P. A. Østergaard, B. Vad Mathiesen, Future district heating systems and technologies: On the role of smart energy systems and 4th generation district heating, Energy 165 (2018) 614–619. URL: https://www.sciencedirect.com/science/article/pii/S0360544218318796. doi:10.1016/j.energy.2018.09.115.

[9] S. Buffa, M. Cozzini, M. D'Antoni, M. Baratieri, R. Fedrizzi, 5th generation district heating and cooling systems: A review of existing cases in Europe, Renewable and Sustainable Energy Reviews 104 (2019). doi:10.1016/j.rser.2018.12.059.

[10] J. von Rhein, G. P. Henze, N. Long, Y. Fu, Development of a topology analysis tool for fifth-generation district heating and cooling networks, Energy Conversion and Management 196 (2019) 705–716. URL: https://doi.org/10.1016/j.enconman.2019.05.066. doi:10.1016/j.enconman.2019.05.066.

[11] L.-S. Wang, Application of exergy: A low-exergy solution to building heating and cooling, in: T. Taner (Ed.), Application of Exergy, IntechOpen, Rijeka, 2018. URL: https://doi.org/10.5772/intechopen.74861. doi:10.5772/intechopen.74861.

[12] G. P. Henze, C. Felsmann, D. E. Kalz, S. Herkel, Primary energy and comfort performance of ventilation assisted thermo-active building systems in continental climates, Energy and Buildings 40 (2008) 99 – 111. URL: http://www.sciencedirect.com/science/article/pii/S0378778807000333. doi:https://doi.org/10.1016/j.enbuild.2007.01.014.

[13] R. Zarin Pass, M. Wetter, M. A. Piette, A thermodynamic analysis of a novel bidirectional district heating and cooling network, Energy 144 (2018) 20–30. doi:10.1016/j.energy.2017.11.122.

[14] I. Sarbu, C. Sebarchievici, A study of the performances of low-temperature heating systems, Energy Efficiency 8 (2015) 609–627. URL: https://doi.org/10.1007/s12053-014-9312-4. doi:10.1007/s12053-014-9312-4.

[15] B. Olesen, Radiant heating and cooling by embedded water-based systems, 2011.

[16] J. D. Feng, S. Schiavon, F. Bauman, Cooling load differences between radiant and air systems, Energy and Buildings 65 (2013) 310 – 321.

URL: http://www.sciencedirect.com/science/article/pii/S0378778813003472. doi:https://doi.org/10.1016/j.enbuild.2013.06.009.

[17] K.-N. Rhee, B. W. Olesen, K. W. Kim, Ten questions about radiant heating and cooling systems, Building and Environment 112 (2017) 367 – 381. URL: http://www.sciencedirect.com/science/article/pii/S0360132316304541. doi:https://doi.org/10.1016/j.buildenv.2016.11.030.

[18] C. F. Reinhart, C. C. Davila, Urban building energy modeling – a review of a nascent field, Building and Environment 97 (2016) 196 – 202. URL: http://www.sciencedirect.com/science/article/pii/S0360132315003248. doi:https://doi.org/10.1016/j.buildenv.2015.12.001.

[19] J. Sokol, C. C. Davila, C. F. Reinhart, Validation of a bayesian-based method for defining residential archetypes in urban building energy models, Energy and Buildings 134 (2017) 11 – 24. URL: http://www.sciencedirect.com/science/article/pii/S037877881631372X. doi:https://doi.org/10.1016/j.enbuild.2016.10.050.

[20] Y. Heo, R. Choudhary, G. Augenbroe, Calibration of building energy models for retrofit analysis under uncertainty, Energy and Buildings 47 (2012) 550 – 560. URL: http://www.sciencedirect.com/science/article/pii/S037877881100644X. doi:https://doi.org/10.1016/j.enbuild.2011.12.029.

[21] C. J. Hopfe, J. L. Hensen, Uncertainty analysis in building performance simulation for design support, Energy and Buildings 43 (2011) 2798 – 2805. URL: http://www.sciencedirect.com/science/article/pii/S0378778811002830. doi:https://doi.org/10.1016/j.enbuild.2011.06.034.

[22] F. Bullo, C. Jorge, D. Florian, M. Sonia, Lectures on network systems, Kindle Direct Publishing, 2019.

[23] L. L. Jensen, D. Trier, M. Brennenstuhl, M. Cozzini, B. Gómez-Uribarri Serrano, D3 . 1 – Analysis of Network Layouts in Selected Urban Contexts, Technical Report, PlanEnergi, 2017.

[24] T. Schluck, P. Kräuchi, M. Sulzer, Non-linear thermal networks - How can a meshed network improve energy efficiency?, CISBAT 2015 Lausanne (2015) 779–785. doi:doi:10.5075/epfl-cisbat2015-779-784.

[25] H. Li, S. Svendsen, District Heating Network Design and Configuration Optimization with Genetic Algorithm, Journal of Sustainable Development of Energy, Water and Environment Systems 1 (2013) 291–303. doi:10.13044/j.sdewes..2013.01.22.

[26] F. Marty, S. Serra, S. Sochard, J.-M. Reneaume, Simultaneous optimization of the district heating network topology and the organic rankine cycle sizing of a geothermal plant, Energy 159 (2018) 1060 – 1074. URL: http://www.sciencedirect.com/science/article/pii/S0360544218309368. doi:https://doi.org/10.1016/j.energy.2018.05.110.

[27] T. Mertz, S. Serra, A. Henon, J. M. Reneaume, A MINLP optimization of the configuration and the design of a district heating network: Academic study cases, Energy 116 (2016) 236–248. doi:10.1016/j.egypro.2017.05.071.

[28] A. Sciacovelli, V. Verda, Topology optimization of robust district heating networks, Journal of Energy Resources Technology 140 (2018) 1–9. doi:10.1115/1.4038312.

[29] T. Falke, S. Krengel, A. K. Meinerzhagen, A. Schnettler, Multi-objective optimization and simulation model for the design of distributed energy systems, Applied Energy 184 (2016) 1508–1516. URL: http://dx.doi.org/10.1016/j.apenergy.2016.03.044. doi:10.1016/j.apenergy.2016.03.044.

[30] B. van der Heijde, A. Vandermeulen, R. Salenbien, L. Helsen, Integrated optimal design and control of fourth generation district heating networks with thermal energy storage, Energies 12 (2019). URL: https://www.mdpi.com/1996-1073/12/14/2766. doi:10.3390/en12142766.

[31] R. E. Best, P. R. Kalehbasti, M. D. Lepech, A novel approach to district heating and cooling network design based on life cycle cost optimization, Energy 194 (2020) 116837. URL: http://www.sciencedirect.com/science/article/pii/S0360544219325320. doi:https://doi.org/10.1016/j.energy.2019.116837.

[32] N. Long, Reduced Order Models for Rapid Analysis of Ambient Loops for Commercial Buildings, Ph.D. thesis, University of Colorado Boulder, Boulder, CO, 2018. URL: https://scholar.colorado.edu/cven{_}gradetdshttps://scholar.colorado.edu/cven{_}gradetds/445.

[33] G. P. Henze, A. G. Floss, Evaluation of temperature degradation in hydraulic flow networks, Energy and Buildings 43 (2011) 1820–1828. doi:10.1016/j.enbuild.2011.03.025.

[34] U.S. DOE, EnergyPlus, 2018. URL: https://energyplus.net, [Accessed 01/12/2018].

[35] U.S. EPA, The difference between source and site energy, 2018. URL: https://www.energystar.gov/buildings/facility-owners-and-managers/existing-buildings/use-portfolio-manager/understand-metrics/difference, [Accessed 01/12/2019].

[36] American Society of Heating, Refrigeration, and Air Conditioning Engineers, Standard 90.1 2013: Energy Standard for Buildings Except Low-Rise Residential Buildings, 2013.

[37] U.S Department of Energy, Commercial prototype building models, 2017. URL: https://www.energycodes.gov/development/commercial/prototype_models, [Accessed 01/12/2019].

[38] R. Strand, C. Pedersen, Implementation of a radiant heating and cooling model into an integrated building energy analysis program, ASHRAE Transactions 103 (1997) 949–958.

[39] C. Chantrasrisalai, V. Ghatti, D. E. Fisher, D. G. Scheatzle, Experimental validation of the EnergyPlus low-temperature radiant simulation, ASHRAE Transactions 109 (2003) 614–623.

[40] COMNET, 2016. URL: https://comnet.org/reference-appendices, [Accessed 26/02/2020].

[41] State of California, Title 24 2013: Building Energy Efficiency Standards for Residential and Non-Residential Buildings, 2012.

[42] R. Hendron, C. Engebrecht, Building America Research Benchmark Definition, 2009.

[43] P. Fanger, Thermal Comfort: Analysis and Applications in Environmental Engineering, Danish Technical Press, 1972.

[44] American Society of Heating, Refrigeration, and Air Conditioning Engineers, HVAC Systems and Equipment, ASHRAE, 2016.

[45] P. D. Lavappa, J. D. Kneifel, Energy Price Indices and Discount Factors for Life-Cycle Cost Analysis – 2015 Annual Supplement to NIST Handbook 135, National Institte of Standards and Technology . U.S Depatrtement of Commerce (2015) 67.

[46] Modelica Association, Modelica language, . URL: https://www.modelica.org/modelicalanguage, [Accessed 20/02/2020].

[47] EURAC Research, Flexynets, . URL: http://www.flexynets.eu/en/, [Accessed 23/02/2020].

[48] J. von Rhein, Modeling, Simulation, and Life-Cost Analysis of Fifth-Generation District Heating and Cooling Networks, 2018.

[49] U.S. Energy Information Administration, U.S. Energy Information Administration - EIA - Independent Statistics and Analysis, 2017. URL: https://www.eia.gov/electricity/?t=epmt56a, [Accessed 14/02/2020].

[50] A. Allen, G. Henze, K. Baker, G. Pavlak, Analysis of HVAC systems for deep energy savings at the urban district level, in: Conference on Sustainable Development of Energy, Water and Environment Systems, Dubrovnik, Croatia, 2019.

[51] American Society of Heating, Refrigeration, and Air Conditioning Engineers, Handbook of Fundamentals, 2017.

[52] J. Kennedy, R. Eberhart, Particle swarm optimization, in: Proceedings of ICNN'95 - International Conference on Neural Networks, volume 4, 1995, pp. 1942–1948 vol.4. doi:10.1109/ICNN.1995.488968.